JACS
JOURNAL OF THE AMERICAN CHEMICAL SOCIETY

ARTICLE

pubs.acs.org/JACS

Fluorescent "Barcode" Multiblock Co-Micelles via the Living Self-Assembly of Di- and Triblock Copolymers with a Crystalline Core-Forming Metalloblock

Feng He,[†,§] Torben Gädt,[‡,§] Ian Manners,[*,‡] and Mitchell A. Winnik[*,†]

[†]Department of Chemistry, University of Toronto, 80 St. George Street, Toronto, Ontario M5S 3H6, Canada

[‡]School of Chemistry, University of Bristol, Bristol BS8 1TS, United Kingdom

Supporting Information

ABSTRACT: We describe the self-assembly in 2-propanol (2-PrOH) of the triblock copolymer, poly(ferrocenyldimethylsilane-*b*-2-vinylpyridine-*b*-2,5-di-(2′-ethylhexyloxy)-1,4-phenylvinylene) (PFS_{30}-*b*-$P2VP_{300}$-*b*-$PDEHPV_{13}$, the subscripts refer to the degree of polymerization). The intense fluorescence of the PDEHPV moieties rendered the resulting cylindrical micelles and their aggregates visible in solution by laser confocal fluorescence microscopy (LCFM). Sonication yielded micelle fragments that could be grown into elongated fiber-like micelles 10 nm in width and nearly monodisperse in length by adding additional block polymer as a solution in tetrahydrofuran. The presence of the conjugated block in the corona promoted slow aggregation of the micelles into hierarchical flower-like structures, but this secondary assembly could be reversed by warming the solution to 50 °C for 30 min. When a solution of 500 nm long micelles of PFS_{30}-*b*-$P2VP_{300}$-*b*-$PDEHPV_{13}$ in 2-PrOH was treated sequentially with controlled amounts of the diblock copolymer PFS_{30}-*b*-$P2VP_{300}$, and in intervals of 24 h, with additional aliquots of PFS_{30}-*b*-$P2VP_{300}$-*b*-$PDEHPV_{13}$, PFS_{30}-*b*-$P2VP_{30}$, and PFS_{30}-*b*-$P2VP_{300}$-*b*- $PDEHPV_{13}$, uniform rod-like multiblock co-micelles were obtained with remarkable optical properties: a banded light-emitting "barcode" structure with fluorescent segments of the triblock copolymer separated by nonemissive segments made up of the diblock copolymer.

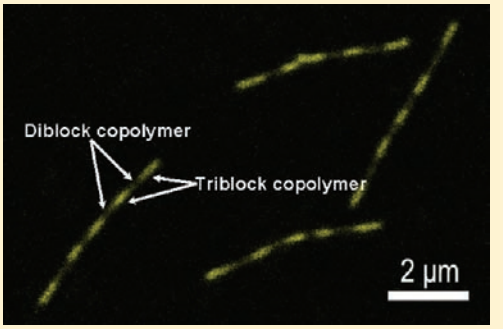

INTRODUCTION

The controlled bottom-up fabrication of nanomaterials with well-defined but complex architectures represents a synthetic challenge of widespread current interest.[1] For many of these applications, it is desirable to prepare the samples as colloidally stable entities. A broad and growing range of different structures can be formed by the self-assembly of block copolymers in solution.[2] Block copolymers are molecules in which polymer chains of different chemical composition are attached at a common junction. Block copolymer self-assembly in solution takes advantage of the fact that certain solvents are good solvents for one (or more) of the polymer chains and a poor solvent for the other polymer chains. The insoluble block undergoes microphase separation and aggregation with other molecules to form the core of micelle-like objects, surrounded by a solvent-swollen corona that provides colloidal stability. Most block copolymers in selective solvents form spherical micelles.

Much of the current interest in block copolymer self-assembly is directed to the formation of more complex structures. For some block copolymer compositions, with carefully chosen solvents, vesicles and cylinders can be formed.[3] Block copolymer vesicles are more robust than traditional liposomes and have a similar range of applications. Cylindrical micelles[4] obtained from the solution self-assembly of block copolymers have found use as additives for the enhancement of the toughness of epoxy resins,[5] as templates for the mineralization of hydroxyapatite[6] or the formation of metal nanoparticles,[7] as materials for flow-intensive drug delivery,[8] and as nanoscopic etch resists.[1g] Recently, even more complex objects have been prepared by self-assembly in solution. These include striped cylindrical structures, toroids, and multicompartmental micelles.[9] When these and other structures are formed by the secondary association of micelle-like building blocks, we refer to this process as "hierarchical" self-assembly.

Additional structural features become prominent when the micelle core consists of a semicrystalline polymer. Early examples in the literature described planar raft-like micelles formed in the solution self-assembly of several different crystalline-coil block copolymers.[10] We reported that poly(ferrocenyldimethylsilane) (PFS) diblock copolymers with a soluble block significantly longer than the organometallic PFS block formed stiff fiber-like micelles, driven by the crystallization of the PFS block in the core.[11] We also found planar structures in selective solvents for polymers in which the soluble block was equal in length or shorter than PFS block, suggesting that curvature imposed by the

Received: March 24, 2011
Published: May 20, 2011

dx.doi.org/10.1021/ja202662u | *J. Am. Chem. Soc.* 2011, 133, 9095–9103

Chart 1

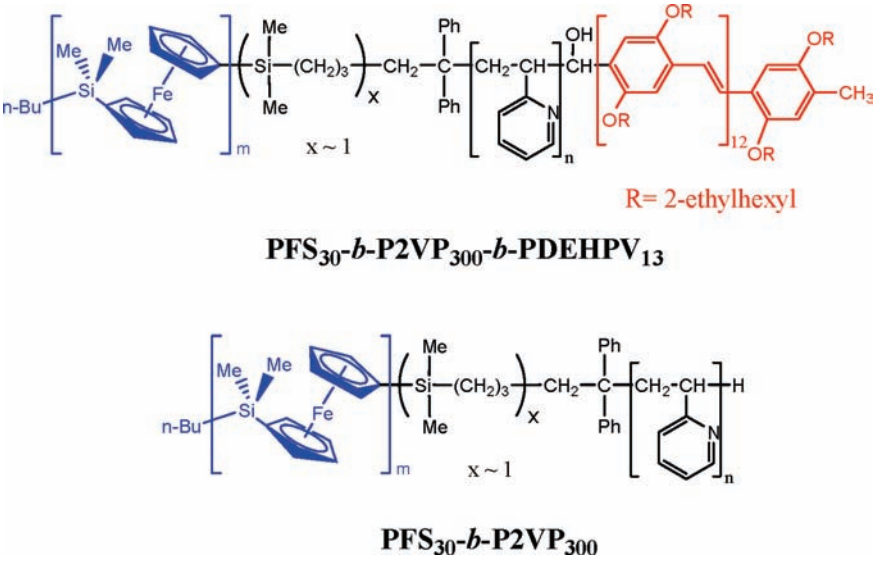

long corona chains plays an important role in determining micelle structure.[12] Recent publications describe other examples of crystalline-coil block copolymers that form cylindrical micelles in selective solvents.[13]

PFS block copolymers are interesting from a number of perspectives. For example, their redox-activity leads to the formation of semiconductive phase-separated nanodomains in the solid-state, and the redox-reversibility has been used to control micelle formation in solution.[14] Recent work has also taken advantage of the ceramization and plasma etch resistance of PFS blocks to fabricate nanostructured surfaces for magnetic data storage and surface-enhanced Raman scattering (SERS) applications.[15] A further, particularly interesting property of PFS block copolymers is that the termini of their cylindrical micelles remain active to the addition of further PFS block copolymer unimers.[16] This novel growth process is apparently driven by epitaxial crystallization of the core-forming PFS block, which can also occur from the edges of platelet micelles and from the surface of crystalline thin films of PFS homopolymer.[17] When these experiments are carried out using very small micelle fragments as seeds, cylindrical micelles with a very narrow length distribution can be obtained. This can be regarded as a living self-assembly process by analogy with classical living covalent polymerizations.[18]

We recently described the synthesis of an ABC block copolymer which combined PFS and a π-conjugated poly(2,5-di(2′-ethylhexyloxy)-1,4-phenylvinylene) (PDEHPV) block, separated by a poly(2-vinylpyridine) (P2VP) middle block, PFS_{30}-*b*-$P2VP_{300}$-*b*-$PDEHPV_{13}$, where the subscripts describe the number average degrees of polymerization.[19] The first two blocks were synthesized by sequential anionic polymerization, followed by quenching of the anionic chain end with the PDEHPV-aldehyde, prepared independently by Siegrist polycondensation.[20] The structures of this triblock copolymer and the corresponding PFS_{30}-*b*-$P2VP_{300}$ diblock copolymer are presented in Chart 1.

When we attempted to prepare micelles of PFS_{30}-*b*-$P2VP_{300}$-*b*-$PDEHPV_{13}$, by heating a sample of the polymer in 2-propanol (2-PrOH) and allowing the solution to cool to room temperature, we did not obtain simple cylindrical micelles. Rather we obtained fascinating rosette-like objects, which at higher magnification in transmission electron microscopy (TEM) images (cf., Figure S1A, Supporting Information (SI)) suggested that these structures were formed by the aggregative assembly of many long fiber-like structures. Because of the fluorescence of the PDEHPV block, we could image these structures in 2-PrOH solution by laser confocal fluorescence microscopy (LCFM, Figure S1B, SI). One of the driving forces for the formation of these aggregates may be the marginal quality of the solvent for the PDEHPV block. 2-PrOH is a poor solvent for PFS and a good solvent for P2VP. We determined a limiting solubility of $PDEHPV_{13}$-CHO in 2-PrOH of 0.02 mg/mL. While the self-assembly experiments were carried out at lower end block concentrations, the local concentration of the PDEHPV block within the micelles may exceed this value and promote aggregation.

In this paper, we present two stories about the self-assembly of PFS_{30}-*b*-$P2VP_{300}$-*b*-$PDEHPV_{13}$ in 2-propanol. In the first story, we show that these flower-like aggregates can be completely disassembled into well dispersed cylindrical micelles of uniform length upon mild warming of the solutions in 2-PrOH. In the second story, we show that using micelle fragments obtained by sonication, and adding sequentially aliquots of PFS_{30}-*b*-$P2VP_{300}$ diblock copolymer and PFS_{30}-*b*-$P2VP_{300}$-*b*-$PDEHPV_{13}$ fluorescent triblock copolymer, each as a solution in tetrahydrofuran (THF), long uniform cylindrical structures can be obtained, with alternating compartments containing nonfluorescent and fluorescent polymer.

Both stories are interesting, but from different points of view. The disassembly of flower-like micelles is a rare, if not unprecedented, example of reversible secondary self-assembly of micelles. The feature that makes this process even more interesting is that the cylindrical structures obtained in this way are uniform in width and have a narrow distribution of lengths. Length distribution is controlled when the initial micelles are formed.

The segmented morphology of the co-micelles obtained from the sequential addition of diblock and triblock copolymer produces structures with compartments of predetermined size, uniform in length. These structures have the properties of one-dimensional submicrometer barcodes[21] that have important applications in the identification of nanosized products with complex physical shapes. By sequential addition of the fluorescent triblock copolymer and nonfluorescent diblock copolymer, light-emitting

periodic barcode nanowires[22] were generated with control of the placement of the fluorescent segments along their length. Even though the fluorescent corona on each bar is only about 40 nm in width, these structures can be read by fluorescence microscopy.

RESULTS AND DISCUSSION

Seeded growth experiments with PFS block copolymer micelles begin with the preparation of a solution of fiber-like micelles followed by sonication. Full experimental details are presented in Supporting Information. For PFS-PDMS micelles (PDMS = polydimethylsiloxane) and PFS-PI micelles (PI = polyisoprene), simple alkane solvents such as hexane and decane serve as selective solvents for the PI or PDMS block. Sonication of these solutions has been used to form micelle fragments. Mild conditions involve relatively brief exposure to an ultrasonic cleaning bath at room temperature.[23] Prolonged or more vigorous sonication conditions can lead to short micelle seeds with a relatively narrow length distribution.[18] A quantitative experiment carried out on $PFS_{48}-PI_{264}$ micelles in decane[24] has shown that the fragmentation rate is very sensitive to the length of the micelles, with k_{frag} increasing as $L_n^{2.6}$, where L_n is the number average length of the micelles.

Seeded growth experiments are normally carried out by adding a few microliters of a solution of a PFS block copolymer in a common good solvent for all blocks, for example, THF, to a diluted solution of the micelle fragments in the selective solvent. When the seeds are themselves small and narrowly distributed in length, the micelles formed are nearly monodisperse in length, with values of L_w/L_n on the order of 1.01−1.05. One of the more remarkable features of this crystallization-driven seeded growth process is that the polymer added during the growth stage can have a different corona chain than that of the seed micelles. For example, cylinders of PFS-PDMS were grown off seed micelles of PFS-PI in hexane and in decane. In one instance, we were able to carry out heteroepitaxial growth experiments in which cylinders of PI-PFG (PFG = poly(ferrocenyldimethylgermane)) were grown off seeds of PFS-PI micelles.[17] Achieving heteroepitaxial growth of one block copolymer with one semicrystalline core-forming block off the ends of micelles with a different semicrystalline core-forming block remains one of the most outstanding challenges in generalizing the concept of seeded micelle growth.

We have referred to the three-component-segment structures obtained by seeded growth as triblock co-micelles. In the work described here, where we describe seeded growth experiments with the diblock copolymer PFS_{30}-*b*-$P2VP_{300}$ and the triblock copolymer PFS_{30}-*b*-$P2VP_{300}$-*b*-$PDEHPV_{13}$, we want to avoid confusion about the term "triblock". In the sections below, when we describe experiments in which PFS_{30}-*b*-$P2VP_{300}$-*b*-$PDEHPV_{13}$ segments are grown off seeds of PFS_{30}-*b*-$P2VP_{300}$, we will refer to the segmented structures obtained as 3-block co-micelles. We will show how we can extend this concept to multiblock structures: 5-block, 7-block, and 9-block co-micelles.

Seeded Growth of PFS_{30}-*b*-$P2VP_{300}$-*b*-$PDEHPV_{13}$ Triblock Copolymer Micelles. In the Introduction, we noted that heating solutions of PFS_{30}-*b*-$P2VP_{300}$-*b*-$PDEHPV_{13}$ in 2-PrOH to 80 °C followed by cooling to room temperature led to the formation of the flower-like structures (cf. Figure S1, SI). Mild sonication of a solution of these structures did not yield micelle fragments suitable for seeded growth experiments. We found, however, that if a solution of the polymer in 2-PrOH (0.05 mg/mL) at 80 °C was immersed directly into the 70 W ultrasonic cleaning bath containing water at 23 °C and sonicated for 10 min, colloidally stable fragments were obtained of uniform width but with a broad length distribution (40−300 nm). This solution was then subjected to prolonged sonication (12 h) at room temperature, after which we obtained seeds (see Figure S2, SI) characterized by L_n = 41.8 nm and L_w/L_n =1.054 (σ/L_n = 0.232, σ: standard deviation).

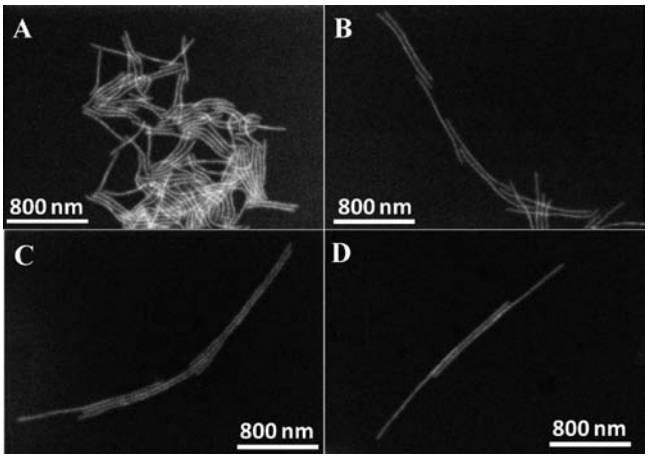

Figure 1. Dark-field TEM image of monodisperse cylindrical micelles of PFS_{30}-*b*-$P2VP_{300}$-*b*-$PDEHPV_{13}$ obtained by adding (A) 500, (B) 1000, (C) 1500, or (D) 2000 μg of triblock copolymer as a THF solution (10 mg/mL) to 50 μg of PFS_{30}-*b*-$P2VP_{300}$-*b*-$PDEHPV_{13}$ seed fragments in 1.0 mL of 2-PrOH.

Starting from this solution of micelle seeds, we prepared long, uniform cylindrical micelles of PFS_{30}-*b*-$P2VP_{300}$-*b*-$PDEHPV_{13}$ by adding more polymer as a solution in THF, a common good solvent for all three components of the triblock copolymer. We added different amounts (500, 1000, 1500, 2000 μg) of the triblock copolymer as a 10 μg/mL THF solution to stirred 2-PrOH solutions (1.0 mL) containing 50 μg of these seeds (0.05 mg/mL). After 10 s, the stirring was stopped, and the samples were allowed to age for 1 day. The resulting micelle solutions were examined by dark-field TEM (Figure 1). In these unstained images, the Fe-rich core of the micelles appears bright. One sees cylindrical micelles of uniform length and a uniform width (10 nm) that is unchanged as the micelles become longer. These micelles have a tendency to aggregate, a topic we will describe in more detail below.

By analysis of these and other images, histograms of length distribution were constructed. These are presented in Figure 2A−D. They indicate that the number average contour lengths (L_n) have values of 485, 920, 1396, and 1845 nm with very narrow length dispersities (L_w/L_n = 1.007−1.016, σ/L_n = 0.084−0.126, Table 1). The most important feature of these results is that the magnitude of L_n is proportional to the amount of triblock copolymer added in the growth step (Figure 2E) and equal to the length predicted if all added polymer condensed on the ends of existing micelles. This type of behavior is consistent with the idea of living epitaxial growth of these micelles: micelle growth with polymeric unimers is analogous to traditional living polymerization in which monomer molecules add to the living ends of a growing polymer chain, and the number of molecules formed in this way depends only on the number of active species that initiate polymerization. For the triblock copolymer examined here, in spite of the length of the P2VP block and the presence of the conjugated block, these polymers assemble to

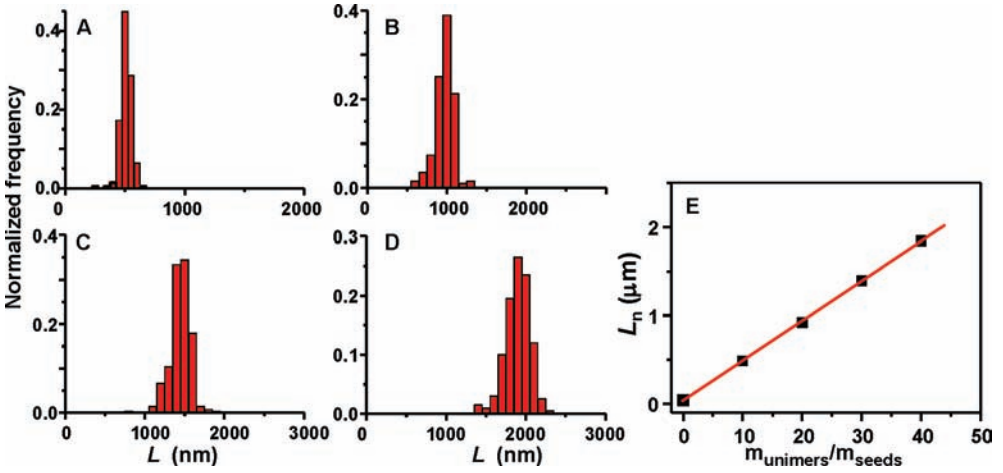

Figure 2. Contour length distributions (CLD) of seeded cylindrical micelles obtained by adding (A) 500, (B) 1000, (C) 1500, or (D) 2000 μg as a THF solution (10 mg/mL) to 50 μg of PFS_{30}-*b*-$P2VP_{300}$-*b*-$PDEHPV_{13}$ seeds in 1.0 mL of 2-PrOH; (e) plot of number average contour length L_n of the PFS_{30}-*b*-$P2VP_{300}$-*b*-$PDEHPV_{13}$ micelles obtained by seeded growth versus the ratio of the mass of added polymer in THF to the mass of the triblock copolymer seeds in 2-PrOH.

Table 1. Length and Polydispersity of Cylindrical PFS_{30}-*b*-$P2VP_{300}$-*b*-$PDEHPV_{13}$ Micelles Obtained by Seeded Growth from Fragments of PFS_{30}-*b*-$P2VP_{300}$-*b*-$PDEHPV_{13}$ Micelles for Different Amounts of Added Polymer

$m_{polymer}/m_{seed}$ [a]	seeds	10:1	20:1	30:1	40:1
L_n (nm) [b]	41.8	485	920	1396	1845
L_w (nm) [b]	44.1	489	934	1407	1857
L_w/L_n	1.054	1.009	1.016	1.008	1.007
σ/L_n [c]	0.232	0.095	0.126	0.089	0.084

[a] Ratio of the mass of triblock copolymer added to that of micelle fragments. [b] L_n, number-average length; L_w, weight-average length. These numbers were obtained by analyzing histogram of the length distribution as shown in Figure 2A−D using the expressions.

$$L_n = \sum_{i=1}^{N} n_i L_i / \sum_{i=1}^{N} n_i \qquad L_w = \sum_{i=1}^{N} n_i L_i^2 / \sum_{i=1}^{N} n_i L_i$$

[c] σ: standard deviation.

$$\sigma/L_n = \sqrt{\frac{L_w}{L_n} - 1}$$

form uniform cylindrical micelles in which the number of micelles is determined by the number of seeds present when the additional polymer is added.

Controlled Disassembly of Aggregated Structures. Attempts to use these samples as templates for further growth were frustrating, and led to fiber-like structures with a broad length distribution. These experiments were carried out several days after the TEM images presented in Figure 1 were obtained. When we took TEM images of the micelle suspensions 5 days after sample preparation, we saw that the micelles had aggregated into large objects with diameters on the order of 5−10 μm. An example is shown in the TEM image in Figure 3A and a laser confocal fluorescence microscopy image of this same sample is presented in Figure 3B. As a potential solution to this problem, we heated solutions of these aggregated micelles at various temperatures and for different periods of time. Heating to 80 °C caused the polymer in the micelles to dissolve. In contrast, heating for 30 min at 50 °C reversed the aggregation, and individual micelles persisted in a colloidally stable

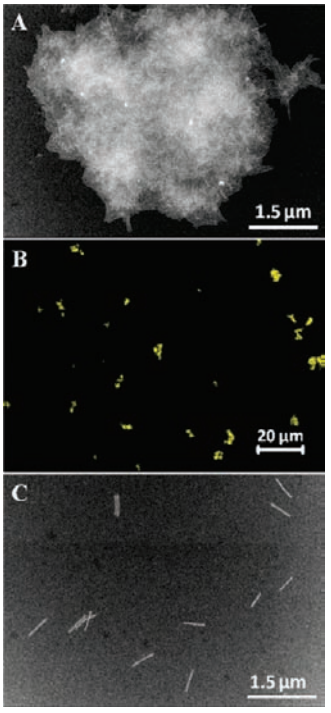

Figure 3. (A) Dark-field TEM image and (B) LCFM image of PFS_{30}-*b*-$P2VP_{300}$-*b*-$PDEHPV_{13}$ micelles (L_n = 485 nm) that aggregated as it was aged for 5 days. The LCFM image was obtained from a ca. 0.1 mm thick solution of the polymer in 2-PrOH; (C) dark-field TEM image of the same sample following heating for 30 min at 50 °C.

state for 10−20 h. Figure 3C presents an example from a TEM grid prepared about an hour after the solution warmed to 50 °C had cooled to room temperature. Comparison of this image with those in Figure 1 leads to the suggestion that some aggregation may have occurred in the samples shown in Figure 1 during the one day of sample aging at room temperature.

Evidence that brief warming completely reverses the consequences of micelle aggregation is provided by the data in Table 2. Here we see that the micelle sample characterized by L_n = 485 nm

Table 2. Mean Length and Polydispersity PFS_{30}-*b*-$P2VP_{300}$-*b*-$PDEHPV_{13}$ Micelles before and after Heating for 30 min at 50 °C

sample history	L_n (nm)	L_w (nm)	L_w/L_n
Before heating[a]	485	489	1.009
Heated at 50 °C for 30 min[b]	477	482	1.010

[a] The sample shown in Figure 2A, after aging 24 h following addition of a solution of polymer in THF to a seed solution in 2-PrOH. [b] Aged for 5 days to form aggregates like those shown in Figure 3A prior to heating.

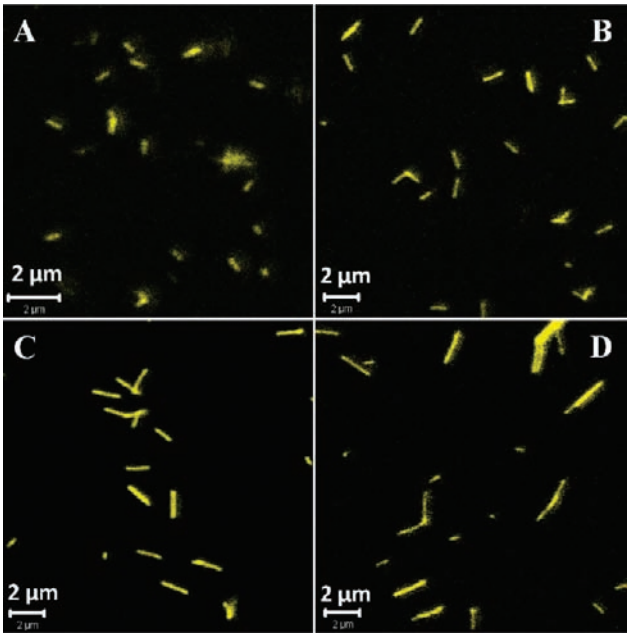

Figure 4. Laser confocal fluorescence images of micelles of PFS_{30}-*b*-$P2VP_{300}$-*b*-$PDEHPV_{13}$ in 2-PrOH obtained by adding (a) 500, (b) 1000, (c) 1500, or (d) 2000 μg as 10 mg/mL THF solutions to 50 μg of PFS_{30}-*b*-$P2VP_{300}$-*b*-$PDEHPV_{13}$ seeds in 2-PrOH. Each sample was heated at 50 °C in an oil bath for 30 min and cooled to 23 °C within an hour of the measurement.

and L_w/L_n = 1.010 as described in Figure 2A emerged from the aggregation-heat-induced deaggregation cycle similar in length (477 nm) and with an equally narrow length distribution.

Figure 4 presents laser confocal fluorescence microscopy images of each of the samples in Figure 2 as solutions in 2-PrOH. These samples had been standing at room temperature in the dark for 5 days, similar to the samples shown in Figure 3 and Table 2. They were then each warmed in an oil bath at 50 °C for 30 min, cooled to room temperature, and examined by LCFM within an hour. Each of the samples shows well-dispersed micelles. Because of the rotational freedom of the micelles in solution, the fluorescence microscope captures micelles at various orientations to the plane of the image. As a consequence, the projected lengths of the micelles in each image are less uniform that in corresponding TEM images, where the micelles lie flat on the TEM grid.

Spectroscopy of PFS_{30}-*b*-$P2VP_{300}$-*b*-$PDEHPV_{13}$ Micelles in 2-PrOH. In our first publication describing the synthesis of PFS_{30}-*b*-$P2VP_{300}$-*b*-$PDEHPV_{13}$,[19] we described the absorption and emission spectra, as well as the fluorescence decay properties of the block copolymer in THF, where the molecules are fully dissolved, and of the rosette-like micelles (cf., Figure S1, SI) in

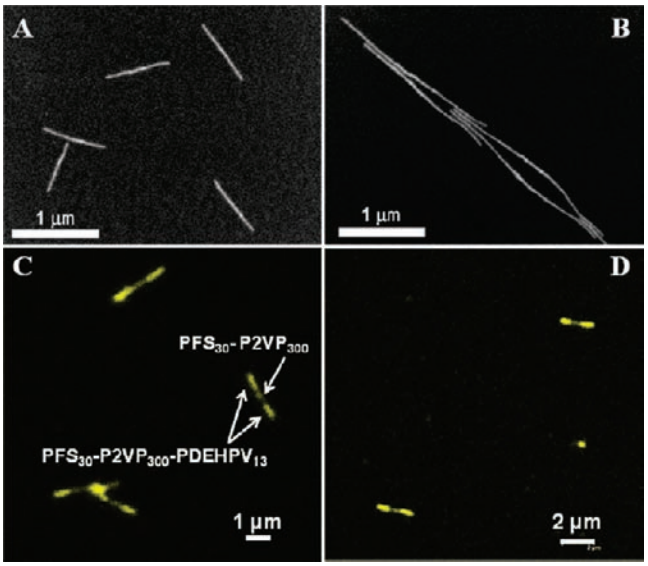

Figure 5. Dark field TEM images of micelles formed (A) by PFS_{30}-*b*-$P2VP_{300}$ in 2-PrOH, and (B) after addition of the triblock copolymer PFS_{30}-*b*-$P2VP_{300}$-*b*-$PDEHPV_{13}$ to form 3-block co-micelles of $M_{PFS30\text{-}b\text{-}P2VP300\text{-}b\text{-}PDEHPV13}$-*b*-$M_{PFS30\text{-}b\text{-}P2VP300}$-*b*-$M_{PFS30\text{-}b\text{-}P2VP300\text{-}b\text{-}PDEHPV13}$. (C and D) CFM images of the 3-block co-micelles in a 100 μm thick solution in 2-PrOH at different magnifications. The solution was heated at 50 °C for 30 min before the measurement.

2-PrOH. In THF, the fluorescence quantum yield of the triblock copolymer was Φ_F = 0.56, which is only slightly less than that of PDEHPV-CHO in THF (0.61). For the triblock copolymer micelles in 2-PrOH, Φ_F = 0.17. Because this value is close to that of PDEHPV-CHO homopolymer in 2-PrOH (Φ_F = 0.18), we imagine that it is the more polar solvent, rather than the self-assembly, that is responsible for the decrease in emission efficiency.

In Figure S3 (SI) we compare the normalized absorbance and emission spectra of solutions of micelles of well-defined length with the spectra of the polymer in THF. We were looking primarily for shifts in λ_{max} and changes in peak shape, rather than quantitative details of the sort reported in ref 19. All of the micelle samples show a peak absorbance at 475 nm, which is very close to that of the triblock polymer in THF (λ_{max} = 474 nm). The main differences among these spectra are the long tail from 550 to 700 nm and the shallower trough in the spectra, which we attribute to a light scattering contribution to the spectra of the micelles. Under UV excitation (365 nm), all of the micelle solutions show very strong green-yellow emission. All of the samples, including the triblock copolymer solution in THF, share a common $\lambda_{max,em}$ = 538 nm with no significant difference in peak shape. We interpret the similarity of the absorbance and emission peaks to indicate that the PDEHPV block in the micelles does not form π-stacked aggregates, which would lead to a red shift in these spectra.

Formation of Multiblock Co-Micelles with Alternating Fluorescent Domains. One of the main conclusions we drew from the LCFM images in Figure 4 was that little aggregation of the micelles occurred in 2-PrOH over short periods of time following warming of the solutions to 50 °C and cooling to room temperature. We took this as evidence that the micelle ends were open, exposed to the solvent, and available for micelle extension. In this way, we designed experiments to generate segmented multiblock co-micelles with alternating fluorescent and dark domains.

dx.doi.org/10.1021/ja202662u |*J. Am. Chem. Soc.* 2011, 133, 9095–9103

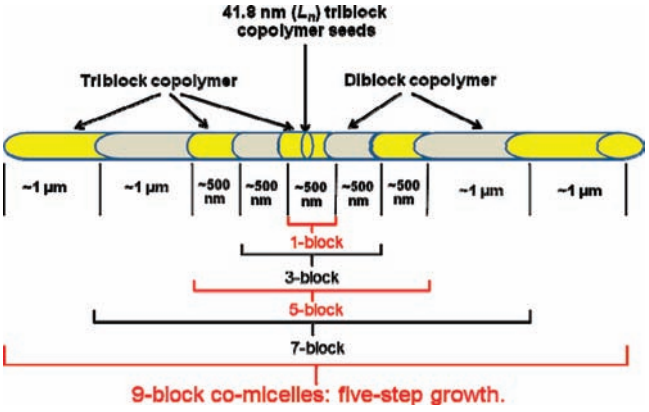

Figure 6. Schematic representation of the formation of 9-block co-micelles (gray, diblock copolymer, PFS_{30}-*b*-$P2VP_{300}$; yellow, triblock copolymer, PFS_{30}-*b*-$P2VP_{300}$-*b*-$PDEHPV_{13}$).

We begin with a description of the preparation of 3-block co-micelles based upon a center segment consisting of PFS_{30}-*b*-$P2VP_{300}$ diblock copolymer. Long micelles of PFS_{30}-*b*-$P2VP_{300}$ were prepared by heating a solution of the polymer in 2-PrOH at 80 °C followed by aging one day at room temperature. This solution was then sonicated at room temperature, yielding seed fragments with L_n = 38.0 nm at a concentration of 0.05 mg/mL. After dilution of 2.0 mL of this seed solution with 4.0 mL of 2-PrOH, 0.1 mL of PFS_{30}-*b*-$P2VP_{300}$ in THF (20 mg/mL) was added under stirring. This amount was designed to grow the micelles to a mean length of ca. 700 nm. After 10 s, the stirring was stopped, and the samples were allowed to age for 1 day. These experiments follow the protocol described in ref 25 for micelles of PFS_{17}-*b*-$P2VP_{170}$. The mean length of the micelles formed in this experiment (Figure 5A) was 750 nm.

This solution was then warmed to 50 °C for 30 min, and an aliquot of PFS_{30}-*b*-$P2VP_{300}$-*b*-$PDEHPV_{13}$ (0.2 mL, 20 mg/mL) in THF solution was added. After brief stirring, the solution was allowed to age one day at room temperature. Epitaxial growth of the PFS triblock copolymer onto the ends of the diblock copolymer micelles led to elongated structures of uniform length with L_n = 2.2 μm as shown in the TEM image in Figure 5B. The increase in length was equal to that expected from the mass of triblock copolymer added and the number of diblock copolymer micelles in the original solution.

The most interesting results are those shown in Figure 5C,D, LCFM images of the micelles in solution, in which one sees only the fluorescence from the PDEHPV component of these structures. In Figure 5C, we identify on the image the dark center segment composed of the diblock copolymer precursor and the end segments composed of the triblock copolymer. On the right-hand side of Figure 5D is a single yellow spot. We attribute this spot to a single micelle oriented perpendicular to the plane of the image. These images provide unambiguous evidence for epitaxial growth of the triblock copolymer onto the ends of the diblock copolymer micelle and show that these block co-micelles are formed as individual colloidal entities in solution.

Multiblocks as Light-Emitting Nanowire Barcodes. Upon the basis of the results shown in Figure 5, we designed experiments to test the possibility of a series of successive growth steps to generate linear rod-like micelles with multiple fluorescent segments. As mentioned in the Introduction, this type of structure would have properties characteristic of light-emitting nanowire barcodes if the lengths of the bright and dark segments could be controlled. Our design protocol is presented in Figure 6. Beginning with the seed micelles shown in Figure S2 (SI), we would generate PFS_{30}-*b*-$P2VP_{300}$-*b*-$PDEHPV_{13}$ with a length of about 0.5 μm. We would then add sufficient amounts of PFS_{30}-*b*-$P2VP_{300}$ to add ca. 0.5 μm of this component to each end. After aging to allow this addition step to come to completion, we would add another aliquot of the triblock copolymer. This would be followed by a second aliquot of diblock copolymer and a third aliquot of triblock copolymer. Prior to each addition step, the solution would be warmed to 50 °C for 30 min and allowed to cool, and subsequent to each addition step, the solution would be allowed to age at room temperature for a day.

To proceed, we began with an aliquot of the micelle solution described in Table 2 with L_n = 477 nm (0.05 mg/mL, 4 mL) as the initial block. After heating the solution 30 min at 50 °C and cooling, we added PFS_{30}-*b*-$P2VP_{300}$ diblock (0.04 mL, 10 mg/mL) in THF. After brief stirring and one day aging, the solution was again warmed at 50 °C for 30 min and then cooled to room temperature. Then half of this micelle solution was reserved for TEM and LCFM experiments, and the other half was used as the mother solution for addition of PFS_{30}-*b*-$P2VP_{300}$-*b*-$PDEHPV_{13}$ (0.02 mL, 10 mg/mL in THF) for the growth of segmented 5-block co-micelles. By repeating this process, we should obtain, in turn, 5-block co-micelles, 7-block co-micelles, and 9-block co-micelles. For the growth of the 3-block and 5-block co-micelles, we controlled to 2:1 the ratio of the mass of added diblock or triblock copolymer in THF to the mass of the initial (1-block) micelles in 2-PrOH solution. For the 7-block and 9-block co-micelles, this ratio was increased to 4:1. As shown in the TEM images in Figure 7, the contour length of these micelles increased in proportion to the amount of new polymer added at each step. Values of L_n obtained by image analysis were 477, 1540, 2390, 4360, and 5920 nm, respectively, after each addition step.

LCFM images of the samples with fluorescent end blocks, as thin solutions in 2-PrOH, are presented in Figure 8. We do not show the samples following addition of the PFS_{30}-*b*-$P2VP_{300}$ diblock copolymer, because these end blocks are invisible by fluorescence microscopy. One can see clearly that the growth steps involving the diblock copolymer introduced dark segments that separated bright segments composed of the fluorescent triblock copolymer. For the 9-block co-micelles, a total of five fluorescent blocks separated by four nonfluorescent blocks can be seen in each micelle as shown in Figure 8C, with the end segments longer, by design, than the three internal fluorescent segments. These images demonstrate the extent of control that we can achieve over the sequential growth steps.

For bar codes to be effective, one has to be able to prepare them in good yield and with good fidelity. The implication of the data in Figure 2 above is that the seeded growth process for these PFS diblock and triblock copolymers occurs with nearly 100% efficiency. When we examine multiple TEM images of the 7- and 9-block co-micelles, we find occasional short fragments. In ref 24, we showed that upon sonication, these long thin micelles fragmented with a rate (k) that increased with contour length L as $k \sim L^{2.6}$. Thus, one might anticipate that as the fiber-like structures become significantly longer, they will increasingly be susceptible to shear-induced fragmentation. As an indication of the uniformity of the structures we obtained during the seeded growth process conceptualized in Figure 6, we present additional TEM images in Figure S4 (SI) of the 7-block co-micelles and in Figure S5 (SI) of the 9-block co-micelles. In Figure S6 (SI), we

dx.doi.org/10.1021/ja202662u |*J. Am. Chem. Soc.* 2011, 133, 9095–9103

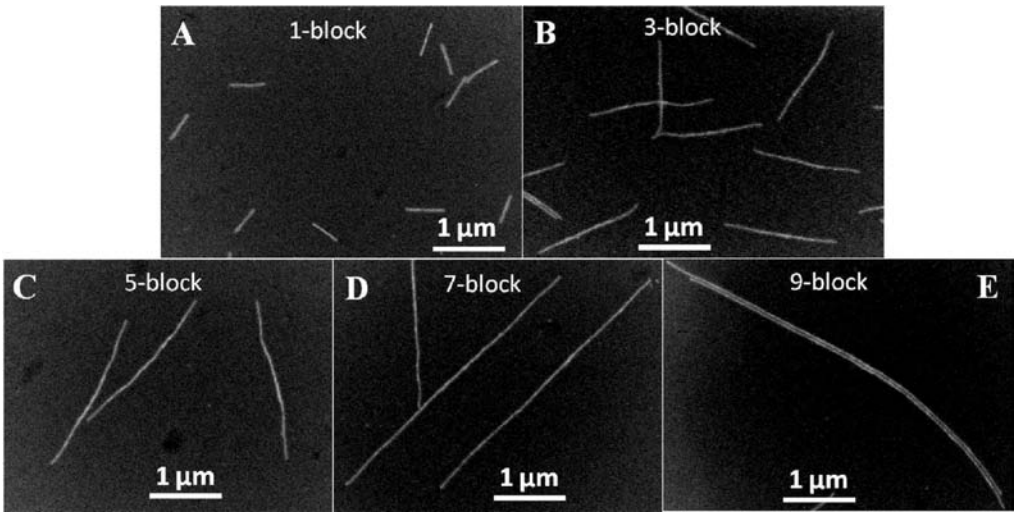

Figure 7. Dark-field TEM images of (A) the initial PFS_{30}-*b*-$P2VP_{300}$-*b*-$PDEHPV_{13}$ micelles, (B) the 3-block, (C) 5-block, (D) 7-block, and (E) 9-block co-micelles obtained by sequential epitaxial growth. Each sample was aged for 1 day, heated 30 min at 50 °C, then cooled to room temperature before preparing the sample on the grid.

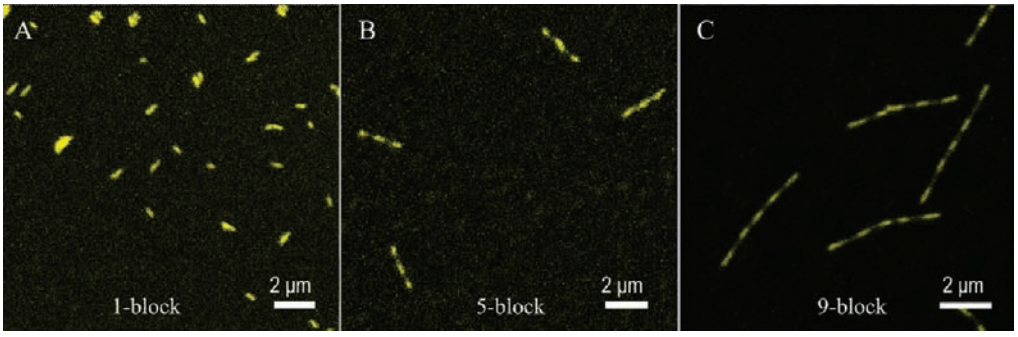

Figure 8. LCFM images of (A) the initial PFS_{30}-*b*-$P2VP_{300}$-*b*-$PDEHPV_{13}$ (1-block) micelles, (B) 5-block and (C) 9-block co-micelles. These image were obtained from thin (0.1 mm) solutions in 2-PrOH. All of solutions were heated at 50 °C for 30 min and then cooled before the measurements.

provide additional LCFM images of the 5-block co-micelles in 2-propanol; and in Figure S7 (SI), of the 9-block co-micelles.

SUMMARY

The experiments described above demonstrate that PFS_{30}-*b*-$P2VP_{300}$-*b*-$PDEHPV_{13}$ can form stiff fiber-like micelles in 2-PrOH solution by a seeded epitaxial growth process that has many features characteristic of the living polymerization of traditional monomers to yield polymer molecules. We find that the number average length increases in proportion to the mass of polymer added to a colloidal suspension of micelle seed fragments, and that the length distribution is exceptionally narrow (L_w/L_n = 1.01). The diblock copolymer PFS_{30}-*b*-$P2VP_{300}$ also forms rod-like micelles in this way, as we reported previously for a shorter diblock copolymer PFS_{17}-*b*-$P2VP_{170}$.[25]

One important difference between these two types of micelles is that the PDEHPV block, presumably at the periphery of the micelle corona, tends to promote micelle aggregation. We know that the synthetic precursor to the triblock copolymer, $PDEHPV_{13}$-CHO, has a limited solubility in 2-PrOH and acts to promote micelle aggregation. One important finding that we report here is that warming aggregated solutions of micelles formed from PFS_{30}-*b*-$P2VP_{300}$-*b*-$PDEHPV_{13}$ at 50 °C for 30 min redispersed the micelles without affecting their length. Micelles redispersed in this way, in dilute solution, remained colloidally stable for 10−20 h.

PDEHPV is highly fluorescent with a quantum yield approaching 20% in 2-PrOH. This property allows the fiber-like micelles that contain this polymer to be visualized by laser confocal fluorescence microscopy. We designed experiments to test the extent to which we could control the epitaxial growth of these PFS block copolymer micelles. In these experiments, starting with rod-like micelles of PFS_{30}-*b*-$P2VP_{300}$-*b*-$PDEHPV_{13}$ with L_n = 477 nm, we carried out stepwise growth experiments, adding carefully controlled amounts, in turn, of PFS_{30}-*b*-$P2VP_{300}$ diblock copolymer and PFS_{30}-*b*-$P2VP_{300}$-*b*-$PDEHPV_{13}$ triblock copolymer. Prior to each addition step, the micelle precursor solution in 2-PrOH was warmed to 50 °C, and after addition of the new polymer in a small volume of THF, the mixture was allowed to age for a day. Solutions were warmed at 50 °C prior to the preparation of samples for TEM or for LCFM measurements. In this way, segmented block co-micelles were obtained. Analysis of the TEM images (cf., Figure 7) indicate that the micelle length after each addition step is that predicted from the mass ratio of the precursor micelle and the new polymer added. As shown in Figure 8, 5-block and 9-block co-micelles possess "barcode" type structures that can be read by laser confocal fluorescence

dx.doi.org/10.1021/ja202662u |*J. Am. Chem. Soc.* 2011, 133, 9095–9103

microscopy. They show very clearly the alternation of bright and dark domains, and the lengths of these domains can be controlled during the micelle growth process.

The segmented nanowires seen in Figure 8 show many of the features of the multicolored luminescent nanowire barcodes reported recently by Park et al.[22] These authors carried out sequential electrochemical polymerization of 3-butylthiophene, 3-methylthiophene, and ethylenedioxythiophene using an aniodic alumina oxide nanoporous template. In this way, they obtained uniform elongated structures, ca. 200 nm in diameter and tens of micrometers in length, in which bar-like segments of the individual polymers could be detected by LCFM through their characteristic fluorescence. The multiblock co-micelles described above are significantly thinner (ca. 40 nm), and represent an interesting and novel example of barcoded nanowires that might provide a useful platform for sensing applications. In the examples that we present here, the barcoded nanowires have light emitting segments with only a single color. We anticipate that, in the future, multicolored segments can be generated by changing the chemical composition of the conjugated polymer in the PFS-P2VP-triblock copolymer, or by attaching fluorescent dyes to the corona forming chains of PFS diblock copolymers.

A further important challenge is to extend living self-assembly to other semicrystalline polymers, especially π-conjugated polymers, in order to access colloidal suspensions of nanowires of controlled length.[13] Such materials would possess useful electronic or optical properties. These types of colloidal nanowires might be patterned by spin coating on substrates structured using electron beam resists and may prove useful as active components in device fabrication.[1g,26]

■ ASSOCIATED CONTENT

Supporting Information. Full experimental details. TEM and LCFM images of the flower-like compound micelles formed on standing, TEM image and length histogram of micelle seeds formed after sonication for 12 h at room temperature, UV−vis and fluorescence spectra of the micelle seeds and of the seeded cylindrical comicelles in 2-PrOH. Additional TEM images of the 7- and 9-block co-micelles, and additional LCFM images of the 5- and 9-block co-micelles in 2-propanol. This material is available free of charge via the Internet at http://pubs.acs.org.

■ AUTHOR INFORMATION

Corresponding Author

mwinnik@chem.utoronto.ca; ian.manners@bristol.ac.uk

Present Addresses

§ For F.H.: Department of Chemistry and The James Franck Institute, The University of Chicago, 929 E. 57th Street, Chicago, IL 60637, USA. For T.G.: BASF Construction Chemicals GMBH, Dr.-Albert-Frank-Str. 32, 83308 Trostberg, Germany.

■ ACKNOWLEDGMENT

F.H. and MAW thank NSERC Canada for their support of this research. I.M. thanks the European Union for a Marie Curie Chair and an Advanced Investigator Grant and the Royal Society for a Wolfson Research Merit Award. T.G. thanks the Deutsche Forschungsgemeinshaft (DFG) for a Postdoctoral Fellowship.

■ REFERENCES

(1) (a) Discher, D. E.; Eisenberg, A. *Science* **2002**, *297*, 967–973. (b) Gohy, J. F. In *Advances in Polymer Science*; Springer-Verlag Berlin: Berlin, 2005; Vol. 190, pp 65−136. (c) Huang, Y.; Duan, X. F.; Cui, Y.; Lauhon, L. J.; Kim, K. H.; Lieber, C. M. *Science* **2001**, *294*, 1313–1317. (d) Hecht, S. *Angew. Chem., Int. Ed.* **2003**, *42*, 24–26. (e) Jain, S.; Bates, F. S. *Science* **2003**, *300*, 460–464. (f) Hu, J. W.; Liu, G. J.; Nijkang, G. *J. Am. Chem. Soc.* **2008**, *130*, 3236–3237. (g) Cao, L.; Massey, J. A.; Winnik, M. A.; Manners, I.; Riethmüller, S.; Banhart, F.; Spatz, J. P.; Möller, M. *Adv. Funct. Mater.* **2003**, *13*, 271–276.

(2) (a) Jenekhe, S. A.; Chen, X. L. *Science* **1999**, *283*, 372–375. (b) Matsen, M. W.; Bates, F. S. *Macromolecules* **1996**, *29*, 7641–7644. (c) Zhang, L. F.; Eisenberg, A. *Macromolecules* **1999**, *32*, 2239–2249. (d) Raez, J.; Manners, I.; Winnik, M. A. *J. Am. Chem. Soc.* **2002**, *124*, 10381–10395.

(3) (a) Zhang, L. F.; Eisenberg, A. *Science* **1995**, *268*, 1728–1731. (b) Zhang, L. F.; Yu, K.; Eisenberg, A. *Science* **1996**, *272*, 1777–1779. (c) Abbas, S.; Li, Z. B.; Hassan, H.; Lodge, T. P. *Macromolecules* **2007**, *40*, 4048–4052. (d) Yuan, J. Y.; Xu, Y. Y.; Walther, A.; Bolisetty, S.; Schumacher, M.; Schmalz, H.; Ballauff, M.; Müller, A. H. E. *Nat. Mater.* **2008**, *7*, 718–722. (e) Zhang, M.; Wang, M. F.; He, S.; Qian, J. S.; Saffari, A.; Lee, A.; Kumar, S.; Hassan, Y.; Guenther, A.; Scholes, G.; Winnik, M. A. *Macromolecules* **2010**, *43*, 5066–5074.

(4) (a) Zhulina, E. B.; Adam, M.; LaRue, I.; Sheiko, S. S.; Rubinstein, M. *Macromolecules* **2005**, *38*, 5330–5351. (b) LaRue, I.; Adam, M.; Pitsikalis, M.; Hadjichristidis, N.; Rubinstein, M.; Sheiko, S. S. *Macromolecules* **2006**, *39*, 309–314.

(5) Dean, J. M.; Verghese, N. E.; Pham, H. Q.; Bates, F. S. *Macromolecules* **2003**, *36*, 9267–9270.

(6) Hartgerink, J. D.; Beniash, E.; Stupp, S. I. *Science* **2001**, *294*, 1684–1688.

(7) (a) Li, Z.; Liu, G. J. *Langmuir* **2003**, *19*, 10480–10486. (b) Yan, X. H.; Liu, G. J.; Haeussler, M.; Tang, B. Z. *Chem. Mater.* **2005**, *17*, 6053–6059. (c) Wang, X. S.; Wang, H.; Coombs, N.; Winnik, M. A.; Manners, I. *J. Am. Chem. Soc.* **2005**, *127*, 8924–8925. (d) Wang, H.; Wang, X. S.; Winnik, M. A.; Manners, I. *J. Am. Chem. Soc.* **2008**, *130*, 12921–12930.

(8) (a) Dalhaimer, P.; Engler, A. J.; Parthasarathy, R.; Discher, D. E. *Biomacromolecules* **2004**, *5*, 1714–1719. (b) Geng, Y.; Dalhaimer, P.; Cai, S. S.; Tsai, R.; Tewari, M.; Minko, T.; Discher, D. E. *Nat. Nanotechnol.* **2007**, *2*, 249–255.

(9) (a) Pochan, D. J.; Chen, Z. Y.; Cui, H. G.; Hales, K.; Qi, K.; Wooley, K. L. *Science* **2004**, *306*, 94–97. (b) Cui, H. G.; Chen, Z. Y.; Zhong, S.; Wooley, K. L.; Pochan, D. J. *Science* **2007**, *317*, 647–650. (c) Li, Z. B.; Kesselman, E.; Talmon, Y.; Hillmyer, M. A.; Lodge, T. P. *Science* **2004**, *306*, 98–101. (d) Zhu, J. T.; Jiang, W. *Macromolecules* **2005**, *38*, 9315–9323. (e) Schacher, F.; Walther, A.; Ruppel, M.; Drechsler, M.; Müller, A. H. E. *Macromolecules* **2009**, *42*, 3540–3548.

(10) (a) Lin, E. K.; Gast, A. P. *Macromolecules* **1996**, *29*, 4432–4441. (b) Richter, D.; Schneiders, D.; Monkenbusch, M.; Willner, L.; Fetters, L. J.; Huang, J. S.; Lin, M.; Mortensen, K.; Farago, B. *Macromolecules* **1997**, *30*, 1053–1068. (c) Vilgis, T.; Halperin, A. *Macromolecules* **1991**, *24*, 2090–2095.

(11) Massey, J. A.; Temple, K.; Cao, L.; Rharbi, Y.; Raez, J.; Winnik, M. A.; Manners, I. *J. Am. Chem. Soc.* **2000**, *122*, 11577–11584.

(12) Cao, L.; Manners, I.; Winnik, M. A. *Macromolecules* **2002**, *35*, 8258–8260.

(13) (a) Portinha, D.; Boué, F.; Bouteiller, L.; Carrot, G.; Chassenieux, C.; Pensec, S.; Reiter, G. *Macromolecules* **2007**, *40*, 4037–4042. (b) Xu, J. T.; Fairclough, J. P. A.; Mai, S. M.; Ryan, A. J. *J. Mater. Chem.* **2003**, *13*, 2740–2748. (c) Chen, C. K.; Lin, S. C.; Ho, R. M.; Chiang, Y. W.; Lotz, B. *Macromolecules* **2010**, *43*, 7752–7758. (d) Mihut, A. M.; Chiche, A.; Drechsler, M.; Schmalz, H.; Di Cola, E.; Krausch, G.; Ballauff, M. *Soft Matter* **2009**, *5*, 208–213. (e) Mihut, A. M.; Drechsler, M.; Möller, M.; Ballauff, M. *Macromol. Rapid Commun.* **2010**, *31*, 449–453. (f) Lazzari, M.; Scalarone, D.; Vazquez-Vazquez, C.; López-Quintela, M. A. *Macromol. Rapid Commun.* **2008**, *29*, 352–357.

(g) Du, Z. X.; Xu, J. T.; Fan, Z. Q. *Macromolecules* **2007**, *40*, 7633–7637. (h) Du, Z. X.; Xu, J. T.; Fan, Z. Q. *Macromol. Rapid Commun.* **2008**, *29*, 467–471. (i) Schmalz, H.; Schmelz, J.; Drechsler, M.; Yuan, J.; Walther, A.; Schweimer, K.; Mihut, A. M. *Macromolecules* **2008**, *41*, 3235–3242. (j) Petzetakis, N.; Dove, A. P.; O'Reilly, R. K. *Chem. Sci.* **2011**, *2*, 955–960. (k) Patra, S. K.; Ahmed, R.; Whittell, G. R.; Lunn, D. J.; Dunphy, E. L.; Winnik, M. A.; Manners, I. *J. Am. Chem. Soc.* published ASAP May 19, 2011, DOI: 10.1021/ja202408w.

(14) (a) Li, J. K.; Zou, S.; Rider, D. A.; Manners, I.; Walker, G. C. *Adv. Mater.* **2008**, *20*, 1989–1993. (b) Eitouni, H. B.; Balsara, N. P. *J. Am. Chem. Soc.* **2006**, *128*, 16248–16252. (c) Rider, D. A.; Winnik, M. A.; Manners, I. *Chem. Commun.* **2007**, 4483–4485.

(15) (a) Lu, J.; Chamberlin, D.; Rider, D. A.; Liu, M. Z.; Manners, I.; Russell, T. P. *Nanotechnology* **2006**, *17*, 5792–5797. (b) Lastella, S.; Jung, Y. J.; Yang, H. C.; Vajtai, R.; Ajayan, P. M.; Ryu, C. Y.; Rider, D. A.; Manners, I. *J. Mater. Chem.* **2004**, *14*, 1791–1794. (c) Hinderling, C.; Keles, Y.; Stöckli, T.; Knapp, H. E.; de los Arcos, T.; Oelhafen, P.; Korczagin, I.; Hempenius, M. A.; Vancso, G. J.; Pugin, R. L.; Heinzelmann, H. *Adv. Mater.* **2004**, *16*, 876–879. (d) Lu, J. Q.; Kopley, T. E.; Moll, N.; Roitman, D.; Chamberlin, D.; Fu, Q.; Liu, J.; Russell, T. P.; Rider, D. A.; Manners, I.; Winnik, M. A. *Chem. Mater.* **2005**, *17*, 2227–2231. (e) Rider, D. A.; Liu, K.; Eloi, J. C.; Vanderark, L.; Yang, L.; Wang, J. Y.; Grozea, D.; Lu, Z. H.; Russell, T. P.; Manners, I. *ACS Nano* **2008**, *2*, 263–270. (f) Lastella, S.; Mallick, G.; Woo, R.; Karna, S. P.; Rider, D. A.; Manners, I.; Jung, Y. J.; Ryu, C. Y.; Ajayan, P. M. *J. Appl. Phys.* **2006**, *99*, 024302.

(16) Wang, X. S.; Guerin, G.; Wang, H.; Wang, Y. S.; Manners, I.; Winnik, M. A. *Science* **2007**, *317*, 644–647.

(17) Gädt, T.; Ieong, N. S.; Cambridge, G.; Winnik, M. A.; Manners, I. *Nat. Mater.* **2009**, *8*, 144–150.

(18) Gilroy, J. B.; Gädt, T.; Whittell, G. R.; Chabanne, L.; Mitchels, J. M.; Richardson, R. M.; Winnik, M. A.; Manners, I. *Nat. Chem.* **2010**, *2*, 566–570.

(19) He, F.; Gädt, T.; Jones, M.; Scholes, G. D.; Manners, I.; Winnik, M. A. *Macromolecules* **2009**, *42*, 7953–7960.

(20) (a) Kretzschmann, H.; Meier, H. *Tetrahedron Lett.* **1991**, *32*, 5059–5062. (b) Olsen, B. D.; Segalman, R. A. *Macromolecules* **2005**, *38*, 10127–10137.

(21) (a) Nicewarner-Peña, S. R.; Freeman, R. G.; Reiss, B. D.; He, L.; Peña, D. J.; Walton, I. D.; Cromer, R.; Keating, C. D.; Natan, M. J. *Science* **2001**, *294*, 137–141. (b) Lee, J. H.; Wu, J. H.; Liu, H. L.; Cho, J. U.; Cho, M. K.; An, B. H.; Min, J. H.; Noh, S. J.; Kim, Y. K. *Angew. Chem., Int. Ed.* **2007**, *46*, 3663–3667.

(22) Park, D. H.; Hong, Y. K.; Cho, E. H.; Kim, M. S.; Kim, D. C.; Bang, J.; Kim, J.; Joo, J. *ACS Nano* **2010**, *4*, 5155–5162.

(23) Massey, J.; Power, K. N.; Manners, I.; Winnik, M. A. *J. Am. Chem. Soc.* **1998**, *120*, 9533–9540.

(24) Guerin, G.; Wang, H.; Manners, I.; Winnik, M. A. *J. Am. Chem. Soc.* **2008**, *130*, 14763–14771.

(25) Wang, H.; Lin, W. J.; Fritz, K. P.; Scholes, G. D.; Winnik, M. A.; Manners, I. *J. Am. Chem. Soc.* **2007**, *129*, 12924–12925.

(26) Massey, J. A.; Winnik, M. A.; Manners, I.; Chan, V. Z. H.; Ostermann, J. M.; Enchelmaier, R.; Spatz, J. P.; Möller, M. *J. Am. Chem. Soc.* **2001**, *123*, 3147–3148.